AIAA 2004-1527

An Asymmetrically-Bistable Monolithic Energy-Storing Structure

M.J. Santer and S. Pellegrino
University of Cambridge, Cambridge, CB2 1PZ, UK

45th AIAA/ASME/ASCE/AHS/ASC Structures, Structural Dynamics, and Materials Conference
19-22 April 2004
Palm Springs, CA

An Asymmetrically-Bistable Monolithic Energy-Storing Structure

M.J. Santer* and S. Pellegrino†
University of Cambridge, Cambridge, CB2 1PZ, UK

The concept of binary robotic systems, in which continuous adaptive behaviour is approximated by the motion of a large number of discrete bistable elements, has created the need for fully-actuated structural bistable elements to be designed and manufactured. This paper discusses potential actuator technologies that could be suitable for such a design, and covers in detail the development, analysis and testing of a jumping bistable device. It is demonstrated that the symmetry of the structure's bistable behaviour has important implications for the selection of driving actuators. Additionally, it is shown that good predictions of the attained jump height, and hence the energy storage characteristics of the element may be made. The monolithic nature of the structure proposed is a distinct advantage over previous structures for integration into a binary robotic system.

Introduction

A novel approach to the design of variable-configuration, or adaptive structures is derived from the concept of binary robotic systems [1], i.e. robots that contain a number of two-state "binary" actuators. The idea is to approximate the continuous shape variation of a conventional adaptive structure by means of a large number of discrete configurations. This approach presents several advantages, in particular the reduction in the need for extensive feedback control: a bistable structural element can only be in one of its two stable states, as any intermediate configuration is unstable, and so a structure made of bistable elements can have only a finite number of configurations. Additionally, there is no requirement for power to be maintained to the actuators in order to hold the structure in any of its configurations. Finally, binary robotic systems can potentially be made from very low-cost components, as is already demonstrated by the existence of a vast number of bistable gadgets that one comes across every day.

In November 2002, a meeting was held between the Deployable Structures Laboratory (DSL) of Cambridge University and the Field Space and Robotics Laboratory (FSRL) of the Massachusetts Institute of Technology (MIT), to discuss advances in the actuation of bistable mechanisms. The outcome of this meeting was the following design challenge, set to both groups: to design and construct a fully actuated bistable structure (of approximately 100 mm × 100 mm), capable of doing useful work over the transition between its stable states. As a demonstration of this ability to do useful work, it was required that the structure be able to jump at least 100 mm from a datum surface. It was also required that this behaviour should be repeatable over a number of cycles.

This paper describes in detail the response of the DSL to this challenge. The paper begins by distinguishing between symmetrically vs. asymmetrically bistable elements, and by presenting an example of a recently proposed monolithic (i.e. joint-less) symmetrically bistable structure. The design process of a jumping structure is then discussed with particular emphasis on the selection of suitable actuators; a novel asymmetrically bistable structure is presented. Next, a detailed analysis of the jump and reset process is presented and, having shown that the proposed structure is able to meet the requirements of the design challenge, a physical prototype of the proposed structure is constructed and tested. A discussion of how the proposed structure might be integrated in a binary robotic system concludes the paper.

Background to Bistable Structures

It is useful to begin with the following definitions: a *Symmetrically-Bistable* structure has equal strain-energy levels in both of its stable states; an *Asymmetrically-Bistable* structure stores a larger amount of strain energy in one of its stable states, and – by releasing this energy – the structure is able to do work over the transition from the higher-energy to the lower-energy stable state.

Initial work on structural bistable elements was carried out by Schiøler [2]. An example of a structure that combines non-linear tape springs with rigid elements – called the four-bar, four-spring mechanism by Schiøler – is shown in Figure 1. This is a closed-loop

*Research Student, Department of Engineering, Trumpington Street.
†Professor of Structural Engineering, Department of Engineering, Trumpington Street. Associate Fellow AIAA. pellegrino@eng.cam.ac.uk

structure consisting of four identical tape springs, i.e. segments of carpenters' steel tape measure, which are widely-used as components of self-locking deployable structures [3], connected to four identical kinked rods. This structure has two stable configurations, in which a pair of opposite tape springs is bent and the other pair is straight. These two configurations are shown in Figure 1. What makes these configurations stable is the much higher stiffness of a straight tape measure, in comparison with a bent one. Because the two

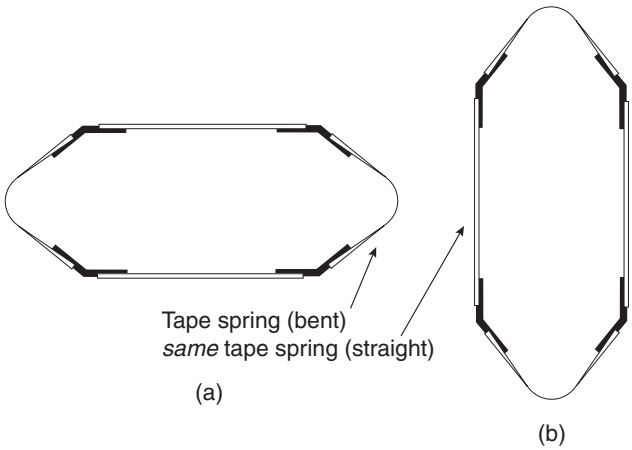

Fig. 1 Two stable configurations of four-bar-four-spring structure.

states Figure 1(a) and Figure 1(b) are geometrically identical, clearly equal amounts of strain energy will be stored in each of these configurations. Hence we are dealing with a symmetrically-bistable structure.

Due to its monolithic nature, i.e. the absence of any sliding parts, the four-bar-four-spring structure was chosen as the starting point for the design of a jumping bistable structure. It should be noted, however, that because this structure is symmetrically-bistable, all the energy for a jump would have to be provided by the actuators effecting the transition between the stable states.

Two potential strategies for actuating a four-bar-four-spring structure are (i) to use an actuator that "pushes" the pair of initially straight tape springs outwards, or (ii) to use an actuator that "pulls" the pair of bent tape spring inwards, as shown in Figure 2.

The force required at the beginning of each actuation phase is considerably larger than later in the process (neglecting the potential force requirement to extend the opposing actuator), as the straight tape springs have to be "buckled" first. Once this has happened, the resistance presented to the driving actuator is considerably reduced, but the actuator has to continue moving the structure towards the alternate stable state, until the other pair of tape spring snap into the straight configuration.

The merits and demerits of these two strategies will be considered as part of the design of the jumping

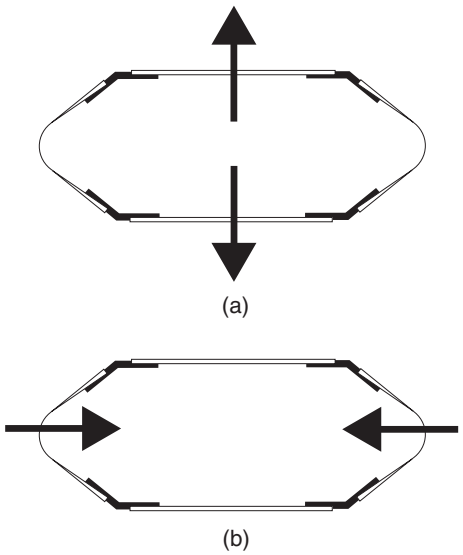

Fig. 2 Two actuation strategies for four-bar-four-spring structure.

bistable structure. First, available actuators will be reviewed to determine for suitability to be integrated with the chosen type of bistable structure. The behaviour of the selected actuator has important repercussions with regards to the design of the structure itself.

Available Actuator Characterisation

In this section, four different actuator technologies will be briefly discussed. The first two, Electro-Active Polymers (EAPs) and Nematic Elastomers, have yet to be used in mainstream applications; the remaining two are established technologies, Shape Memory Alloy (SMA) and piezo-electric ceramic. For each type of actuator, the working principle will be explained, and issues relevant to their suitability for the present application will be assessed.

EAP Actuators

An EAP is any compliant elastomeric polymer with a high dielectric constant (the ratio of the polymer permittivity to the permittivity of free space). When coated with a compliant electrode on both faces and subject to a potential difference, an effective pressure, known as the Maxwell stress, is produced by the electrodes on the film [4, 5]. This pressure p may be expressed as a function of the applied electric field E, and hence the potential difference between the electrodes V and film thickness t, as

$$p = \epsilon_r \epsilon_0 E^2 = \epsilon_r \epsilon_0 \left(\frac{V}{t}\right)^2 \tag{1}$$

The product $\epsilon_0 \epsilon_r$ is the permittivity of the polymer. Under this pressure, shown in Figure 3, the polymer compresses in the 3-direction, and by conservation of volume must expand in the 1 and 2-directions, to a

greater or lesser extent depending on the elastic properties of the polymer.

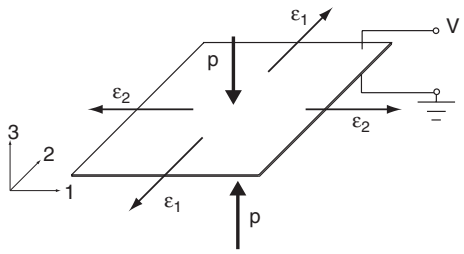

Fig. 3 EAP deformation under Maxwell Stress

It may be seen from Equation 1 that it is desirable to have the film thickness as small as possible in order to maximise the Maxwell stress for a given electric field. A very promising film is VHB-4910 tape manufactured by 3M. As manufactured, however, the VHB-4910 tape is 1 mm thick. This is far too thick to allow a sufficient Maxwell stress to be induced without exceeding the critical breakdown voltage for the material. In order to use the tape as a viable actuator material, the material must be prestrained to reduce the thickness. The visco-elastic nature of the acrylic means that the stress induced by the prestrain quickly relaxes.

A major issue concerning the fabrication of EAP actuators is the choice of material for the compliant electrodes. They must be robust enough to endure electric fields of hundreds of kV/mm and maintain a good electrical contact when stretched. Potential solutions are Carbon or Silver grease, which however show a tendency to crack when they dry out over time; and Carbon powder, which, whilst reasonably effective, relies on the adhesion properties of the EAP film itself.

As the dominant actuation mode of EAP's is lateral expansion, as shown in Figure 3, and the thin EAP film cannot withstand compressive forces without buckling, it is necessary to devise a means for the EAP film to act in a tensile mode.

The development of an EAP actuator specifically for integration into a binary robotic structure is the focus of ongoing research at the FSRL [6]. The FSRL approach is to have layers of EAP within a mechanism consisting of rigid elements connected with compliant hinges. Several working prototypes of Electro-active Polymer Artificial Muscles (EPAMs) have been made. Current prototypes exhibit large strains up to 200% and an available force of ten times the weight of the device. They also exhibit the high specific energy and efficiency that is characteristic of EPA devices. Their force to weight ratio, however must still be improved before they become viable for the actuation of bistable structures.

Nematic Elastomer Actuators

Nematic elastomers exhibit coupling between rubber elasticity and liquid-crystalline degrees of freedom [7]. This effect can result in a number of unusual properties, but it is their ability to exhibit considerable strains in response to an increase in temperature, or exposure to light, that makes them attractive for use in actuators. Nematic rubbers may be made with an infinite number of properties, but the ultimate tensile stress is usually of the order of 0.1 MPa; the actuation temperature can be varied, but it is usually below 100°C.

Compressive strains of up to 50% are readily achieved, which makes nematic elastomers particularly attractive for the actuation of bistable mechanisms. A considerable advantage is that when the temperature is lowered below the actuation threshold the actuator returns to its original configuration. This means that if two nematic actuators were attached to the structure of Figure 2, in orthogonal directions, in any cycle the driving actuator would be getting shorter while the other actuator is slack.

As their production technology improves, nematic elastomers are likely to become a very promising technology for the present application, although this stage has yet to be reached.

Amplified Piezo-electric Actuators

Piezo-electric materials are capable of generating high forces, but only low strains, typically of the order of 0.01%. Amplified Piezo-electric Actuators (APAs), consisting of multi-layered piezo-electric elements surrounded by a motion-amplifying frame, have been developed by Cedrat Technologies [8]. The highest stroke available at present is 500 μm with a blocked force of 570 N from the APA500L actuator, which is 55 mm high. These properties correspond to an equivalent strain of the order of 1%.

The effective stroke may be further amplified by stacking APAs in series, but the equivalent strain of this type of actuator is just too small for the present application. Bistable structures such as the four-bar-four-spring structure undergo equivalent strains in excess of 100% between opposite points connected by an actuator in Figure 2.

An important issue, though, is whether the actuators need to remain attached to the structure while it moves. Clearly all that is required is to take the structure past the configuration of maximum strain energy; provided that the strain energy decreases monotonically from this point onwards. After reaching this point, one end of the actuator could simply detach itself and the motion would continue. In the case of symmetrically-bistable structures, this intermediate point cannot occur before half-way between the two stable configurations and hence an actuator capable of delivering at least 50% strain would be required. In the case of asymmetrically-bistable structures, only a very small equivalent strain is usually sufficient to initiate the motion from the higher energy state. It

would not be possible, however, to actuate the reverse cycle with an APA.

SMA Actuators

Shape Memory Alloys display the so-called shape memory effect, which is associated with a reversible thermoelastic transformation between austenitic and martensitic phases within the alloy [9]. This effect is exhibited by many alloys, but Nickel-Titanium (NiTi) wire is the most readily available. NiTi may be trained into a particular shape through heat treatment. Following this process, any deformations that the wire is subjected to, within its allowable strain limits (beyond which permanent, i.e. plastic deformation occurs), may be recovered by heating it above its transformation temperature.

A 0.5 mm diameter wire is capable of generating a stress of up to about 650 MPa while recovering strains of up 8%. A considerable increase in the equivalent recoverable strain, without increasing the material strain, can be achieved by forming a NiTi wire into a helical spring. NiTi springs of this type are manufactured by Mondotronics Inc. [10] which have a stroke of 110 mm against a blocking force of over 30 N. A photograph of spring model 3-642 in the two extreme configurations is shown in Figure 4.

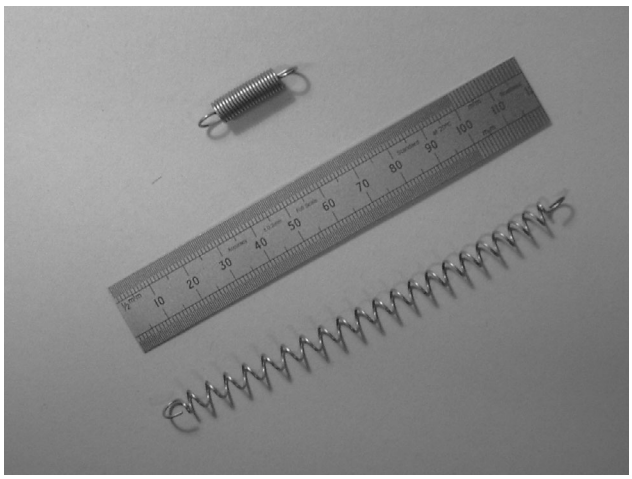

Fig. 4 Extreme configurations of Mondotronics NiTi spring.

A quasi-static experiment was carried out on these springs in order to characterise them for design purposes. This experiment determined the maximum available blocked force for the corresponding extension of the NiTi spring

The quasi-static experiment was carried out according to the following procedure. The spring was extended by 60 mm in an Instron-5564 materials testing machine, and held in this configuration. The spring was insulated from the machine, both electrically and thermally, by means of Kevlar chords, and then heated by passing a current of 2 Amps through its full length. Heating initiates the austenite transformation, which causes the spring to attempt to contract. As this contraction is prevented by the Instron, a force is exerted by the spring on the Instron. With the spring being maintained in its heated state, the jaws of the Instron were moved closer at a rate of 0.02 mm/s, to measure the available force over the full range of extension. The results of this experiment are plotted in Figure 5.

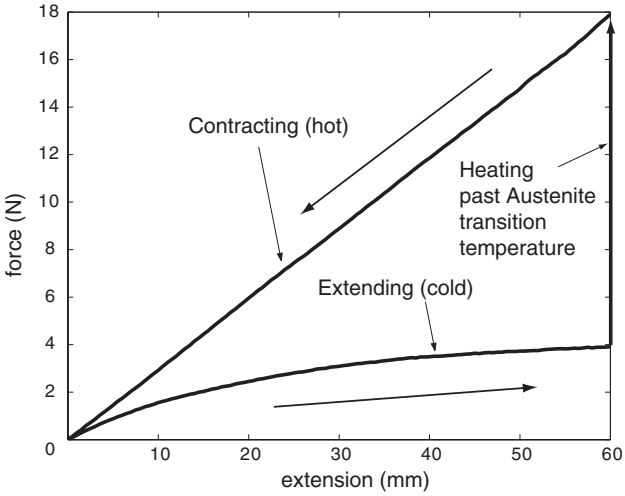

Fig. 5 NiTi spring quasi-static experiment results.

It can be seen that when the spring is extended cold, it behaves in a non-linear fashion that is a combination of the linear-elastic behaviour of the spring plus the plastic-like transformation of the martensite microstructure. When the spring is heated past the austenite transition temperature, it behaves exactly like a linear spring, but generates a force considerably greater than that required for the extension. The available energy is represented by the area bounded by the extension and contraction curves. It must be noted that the experiment presented in Figure 5 did not go up to the maximum 110 mm extension, but the behaviour in this case would be substantially identical.

This experiment shows that NiTi springs are (i) able to recover fully an initial extension and (ii) behave linear-elastically, when in a heated state. It is useful to represent functionally the behaviour of the NiTi spring. It is noted that the force-extension behaviour of a cold NiTi spring tends to an approximately constant value.

Therefore, the following expressions may be used to describe the behaviour of the Mondotronics NiTi springs

$$\text{ON} \qquad F \approx 333.3\, x \tag{2}$$

$$\text{OFF} \quad F \approx \begin{cases} 18.2\, x^{0.52} & (0 \le x \le 0.06) \\ 4 & (x > 0.06) \end{cases} \tag{3}$$

in which x is the extension of the spring, in metres, measured from the contracted state, and F, in Newtons, is the actuation force.

Discussion

In order to actuate bistable structures successfully, ideally both high force and long stroke should be available in the chosen actuator. Actuators that work in tension are thought to be advantageous. Of the technologies discussed above, SMA springs appear the closest to these ideals if off-the-shelf availability is required. EAP and Nematic Elastomer technologies show great potential, but there are a number of design issues to overcome before they can become a viable option.

Asymmetrically-Bistable Structure

None of the available actuator technologies has a sufficient power output to cause a structure to jump in the manner set out in the design challenge. Therefore, it is necessary for the structure itself to provide the power required for the jump and so an asymmetrically-bistable version of the four-bar-four-spring structure shown in Figure 1 was considered.

The basic concept is shown in Fig. 6. One pair of tape springs has been replaced with regular flat leaf springs, which have a linear moment/rotation relationship, in order to remove the symmetric behaviour of the original structure. The actuation strategy, also shown in the figure, involves a single actuator that triggers the jump, Figure 6(a), and a symmetric pair of actuators to take the structure back into its higher-energy configuration, Figure 6(b). Two further changes have been made to improve the jumping characteristics: the included angle of the corner pieces has been changed from obtuse to acute, with the effect that two points will push off against a base support, instead of only one point, and the corner pieces have been extended outwards, to amplify the push-off action and also to provide an attachment point for the resetting actuators.

The first stage of the design process involved optimising the geometry of the structure to maximise the available jumping energy for given (leaf and tape) spring characteristics. A tape spring may be idealised as behaving linearly up to a critical snapping moment, and providing a constant moment, M^*, thereafter [11]. For a given leaf spring, the spring constant K may be calculated by making the approximation that the loading condition is pure moment applied at each end. Making the additional assumption that there is zero strain on the neutral axis at all times, requires that the leaf spring deform as a developable surface, i.e. a circular arc [12].

Thus the geometry of the whole structure and hence the curvature κ of the leaf spring may be determined for every intermediate position between the stable states. The moment exerted by the leaf spring for any given geometry may be calculated from

$$M_{\mathrm{LS}} = D\kappa \qquad (4)$$

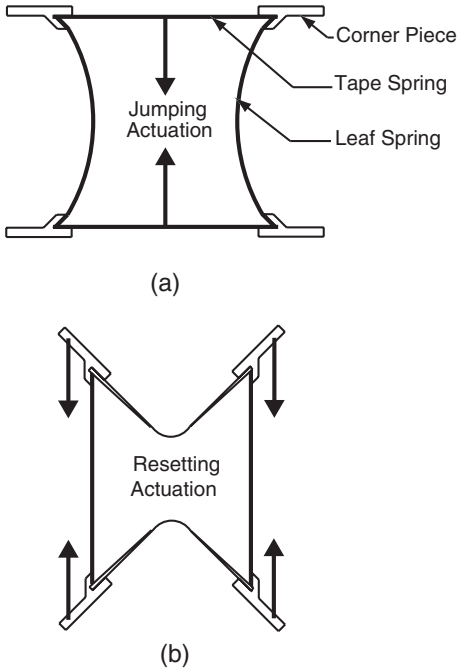

Fig. 6 Concept of jumping structure (a) higher-energy configuration and (b) lower-energy configuration.

in which D is the plate bending stiffness (used because the width/thickness ratio of 36.6 for the leaf spring that will be used is more indicative of a plate than a beam).

To ensure that the structure is able to lock in the configuration of higher energy, the maximum moment exerted by the leaf spring must be less than the maximum moment that can be carried by the tape spring. A margin of 15% was enforced in the design. For the available tape and leaf springs, a fixed corner angle $\alpha = 55^\circ$ was the nearest integer to the value that maximises the energy available for jumping, subject to this constraint.

A plot of the moments acting on a corner of the structure is shown in Figure 7, where ψ represents the rotation of the corner during the transition between the two stable states. The available energy for a jump is the area bounded by the curves.

A simple upper-bound prediction for the height attained in a jump, may be made by assuming that all stored energy is converted into the potential energy of the structure corresponding to this height. In the case where the energy absorbed by the resetting actuators is negligible (as would be the case, for example, if nematic elastomer actuators were used), the available energy is represented by the area bounded by the curves in Figure 7. In the case where the resetting actuators absorb a considerable amount of energy (as when NiTi Springs are used) this must be included in the calculations.

These predicted heights are as follows. In the case

where the resetting actuators are neglected the available jumping energy is 0.34 J, corresponding to a potential height of 0.498 m. Resetting two Mondotronics springs absorbs 0.21 J, corresponding to a potential height of 0.186 m.

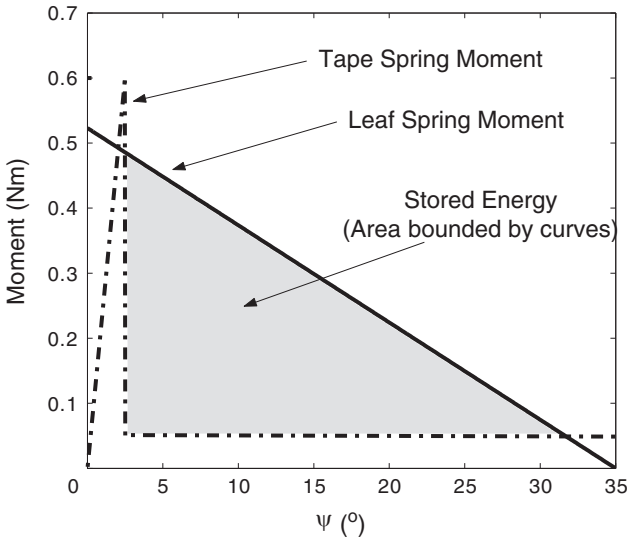

Fig. 7 Moments acting on a corner of the asymmetrically bistable structure.

Reset Analysis

Having designed an asymmetrically-bistable structure that maximises the available jumping energy, the behaviour of the structure during its reset cycle may be analysed as follows.

Consider the structure in a general configuration between the two stable states, as shown in Figure 8. This configuration is fully defined by the corner rotation from the horizontal, ψ. Note that each tape spring is idealised as two rigid parts of length $b/2$, connected by a hinge. Also note that, since $\theta = \pi - 2\psi - 2\alpha$, the curvature of the leaf springs is given by

$$\kappa = \frac{\pi - 2\alpha - 2\psi}{a} \tag{5}$$

The structure is in quasi-static equilibrium under the action of pairs of equal and opposite forces applied by the actuators, which we will think of as external forces. Gravity effects will be neglected.

Figure 9(a) shows free-body diagrams for the corner elements and the two types of springs. Note that each spring is subject to a uniform bending moment, which is the constant M^* in the tape spring and the curvature-dependent M_{LS} in the leaf spring. Figure 9(b) shows the configuration change associated with a small corner rotation $d\psi$.

Equating internal to external virtual work gives the following equation of equilibrium

$$4M^* d\psi - 4M_{\mathrm{LS}} d\psi = 2F_1 dx_1 + 4F_2 dx_2 \tag{6}$$

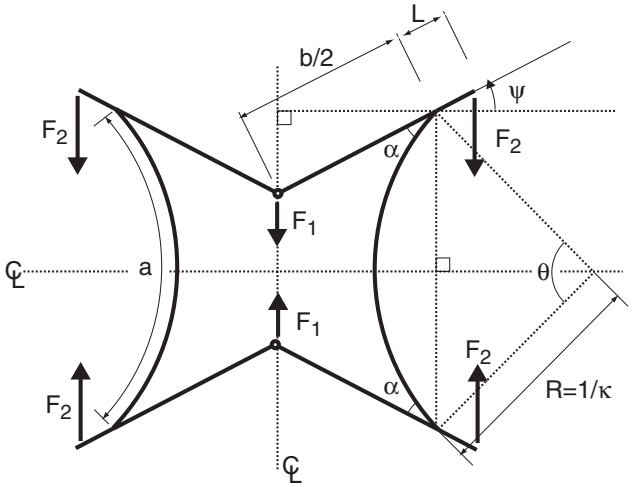

Fig. 8 General configuration during reset cycle.

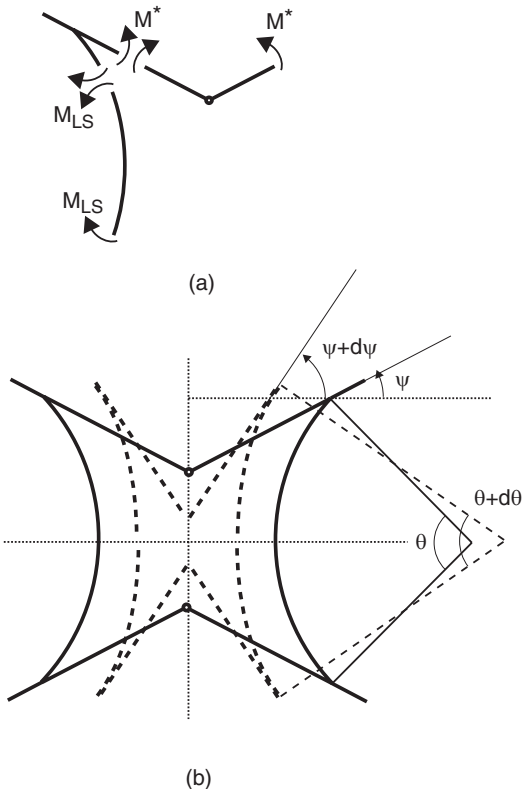

Fig. 9 (a) Stress resultants during reset; (b) small change of configuration.

The work done by the actuators, on the right-hand-side of Equation 6, is given by the product of the actuator force and the change of distance between the points connected by the actuator. The values of the actuator forces can be obtained from Equations 3,2. If we define a positive change to be an increase in distance, dx_1 and dx_2 may be obtained by differentiation,

with respect to ψ, of

$$x_1 = \frac{2a}{\pi - 2\alpha - 2\psi} \sin \frac{\pi - 2\alpha - 2\psi}{2} - b \sin \psi - l_0 \quad (7)$$

$$x_2 = \frac{2a}{\pi - 2\alpha - 2\psi} \sin \frac{\pi - 2\alpha - 2\psi}{2} + 2L \sin \psi - l_0 \quad (8)$$

in which x_1 and x_2 are the instantaneous lengths of the central and outer actuators respectively, and l_0 is the unextended actuator length.

Making the substitutions indicated above, eliminating $d\psi$ and rearranging, Equation 6 becomes

$$4M^* - \frac{4D}{a}(\pi - 2\alpha - 2\psi) - F_1^{OFF} b \cos \psi + 4F_2^{ON} L \cos \psi = 0 \quad (9)$$

Using the experimentally determined actuator profiles (Equations 2 and 3), and $M^* = 50$ Nmm, the minimum resetting actuator force profile may be plotted for every stage of the cycle as in Figure 10. The slight discontinuity in the curve is due to the functional approximation of the NiTi springs, and is not a real feature. It may be seen the NiTi spring actuators

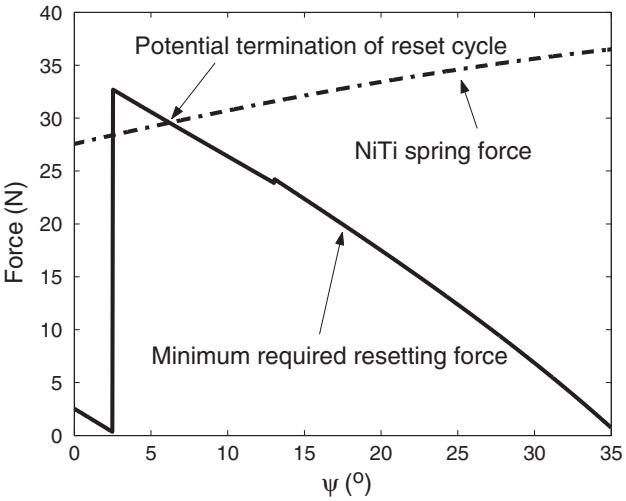

Fig. 10 Mimimum resetting actuation force profile

appear insufficient to perform this function, predicting a termination of the reset cycle at an angle $\psi = 6.1°$. The reason that these actuators may still be used is covered in the Experimental Observations section.

Dynamic Jump Analysis

To estimate the initial conditions before the structure takes off, during a jump, a full dynamic analysis of the motion up to the point where the structure loses contact with the ground is described below for the case when resetting actuators are neglected.

The analysis begins at the time when the structure has just abandoned its high energy stable state. The notation used in the analysis is shown in Figure 11.

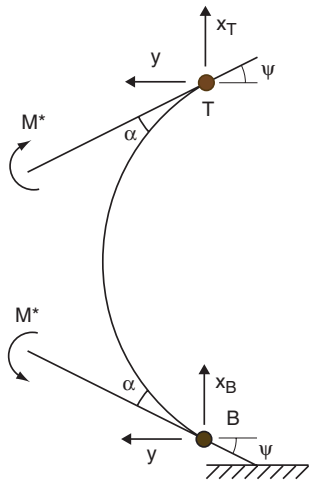

Fig. 11 Notation used for analysis of jump.

By symmetry, only half of the structure is considered.

T and B denote the points of intersection of the centre lines of the tape springs and the leaf springs. A lumped mass m with moment of inertia J is assumed at each of these points. The vertical components displacement of these points, from the configuration in which $\psi = 0$, are x_T and x_B, and the horizontal component is y.

The equation of motion can be obtained by virtual work, considering the set of virtual displacements already used for the reset analysis, see Figure 9(b). Clearly, the work done by the D'Alembert forces needs to be included in the present case. Virtual work gives

$$2M_{\mathrm{LS}} d\psi + 2M^* d\psi + m\ddot{x}_T dx_T + m\ddot{x}_B dx_B + 2m\ddot{y} dy + 2J\ddot{\psi} d\psi = 0 \quad (10)$$

The linear displacements x_T, x_B and y are related to the angular displacement ψ by assuming a circular deformation of the leaf spring resulting in

$$x_T = \frac{a}{\frac{\pi}{2} - \alpha - \psi} \sin\left(\frac{\pi}{2} - \alpha - \psi\right) - \lambda + L \sin \psi \quad (11)$$

in which

$$\lambda = \frac{a}{\left(\frac{\pi}{2} - \alpha\right)} \sin\left(\frac{\pi}{2} - \alpha\right)$$

and

$$x_B = L \sin \psi \quad (12)$$

$$y = \left(L + \frac{b}{2}\right)(1 - \cos \psi) \quad (13)$$

In order to be solved, this equation must be rewritten in terms of a single variable. It turns out that ψ is the most convenient to choose. It can be shown that

$$\ddot{x}_T = \frac{\partial x_T}{\partial \psi} \ddot{\psi} + \frac{\partial^2 x_T}{\partial \psi^2} \dot{\psi}^2 \quad (14)$$

and similarly for x_B and y. Substituting these expressions allows the equation of motion to be written in the form

$$A(\psi)\ddot{\psi} + B(\psi)\dot{\psi}^2 + C(\psi) + 2M^* = 0 \qquad (15)$$

in which

$$\begin{aligned} A &= 2J + m\left[\left(\frac{\partial x_T}{\partial \psi}\right)^2 + \left(\frac{\partial x_B}{\partial \psi}\right)^2 + 2\left(\frac{\partial y}{\partial \psi}\right)^2\right] \\ B &= m\left(\frac{\partial x_T}{\partial \psi}\frac{\partial^2 x_T}{\partial \psi^2} + \frac{\partial x_B}{\partial \psi}\frac{\partial^2 x_B}{\partial \psi^2} + 2\frac{\partial y}{\partial \psi}\frac{\partial^2 y}{\partial \psi^2}\right) \\ C &= 2\frac{D}{a}(\pi - 2\alpha - 2\psi) \end{aligned}$$

Equation 15 was solved numerically using Matlab [13]. The lumped mass was taken to be a quarter of the total, $m = 17.5$ g, and the value of j was calculated as the inertia of a single corner piece, $J = 0.547 \times 10^{-6}$ kgm^2.

Using these values, the plots shown in Figure 12 and Figure 13 were obtained for the linear and angular displacements and velocities for the structure over the transition between the less preferential and the preferential stable states. For simplicity, take-off – which

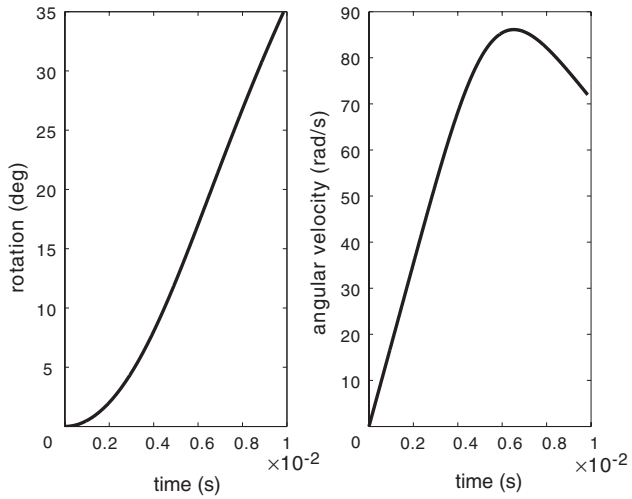

Fig. 12 Angular motion between snap and jump.

occurs when the contact force between the feet of the structure and the ground becomes zero – is assumed to occur at the time when the lower energy stable state is reached. In fact, take-off occurs slightly later, and the delay depends on the length of the extension on the feet.

The analysis predicts a rigid body velocity at the point of take-off of 1.475 ms^{-1}. Then it is straightforward to determine the jump height, as a particle with initial, vertical velocity v and subject to constant acceleration g reaches a height

$$s = \frac{v^2}{2g} \qquad (16)$$

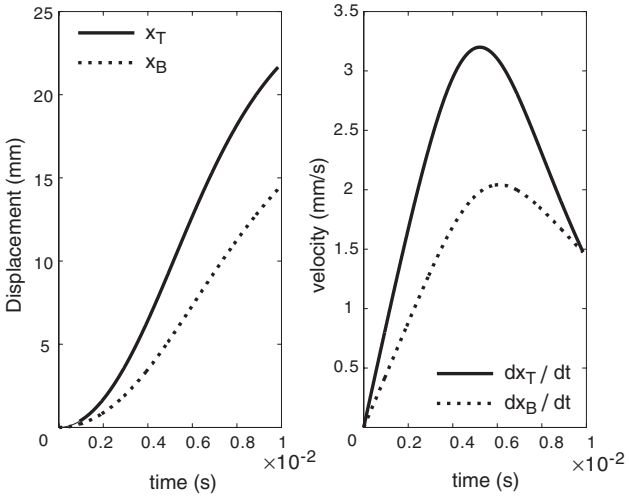

Fig. 13 Vertical displacements and velocities between snap and jump

For $v = 1.475$ ms^{-1} Equation 16 predicts a height $s = 0.111$ m. This analysis represents a considerable improvement over the energy analysis described in the Section Asymmetrically-Bistable Structure, which shows that the effects of rotational inertia of the jumping structure cannot be ignored.

Experimental Observations

Several jumping and reset experiments were carried out and recorded with a digital video camera. Figure 14 shows stills from two of the movies from the experiments, when the structure is at its maximum height. Although the images are rather blurred, the height reached by the centroid can be measured with reasonable accuracy.

Figure 14(a) shows a typical experiment, the height attained was $s = 0.145$ m. Figure 14(b) shows an experiment in which the resetting actuators had been prestretched before activating the jumping actuator, so that they would only contribute to the mass of the structure, but not absorb any energy. Hence a greater jump height of $s = 0.163$ m was achieved. In this case extensive internal vibration of the structure was observed in the movie. The predicted and experimentally observed jump heights are listed in Table 1.

	Method	**Jump**
Without Resetting Actuators	Energy Analysis	0.498 m
	Dynamic Analysis	0.111 m
	Experiment	0.163 m
With Resetting Actuators	Energy Analysis	0.186 m
	Experiment	0.145 m

Table 1 Comparison of predicted and observed jump heights

The electric current required to actuate the NiTi springs must be commented upon. For the jump cycle the rated current of 2 Amps was sufficient to trip the

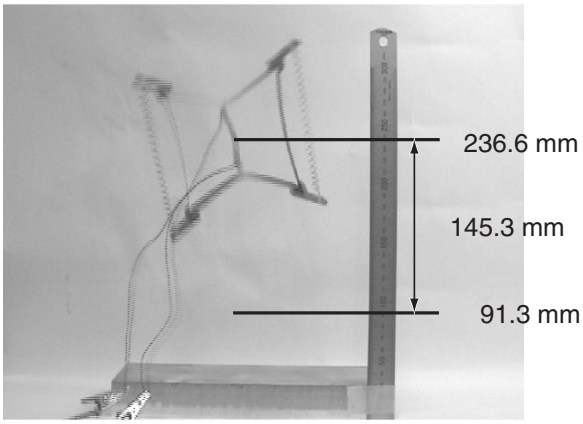

(a)

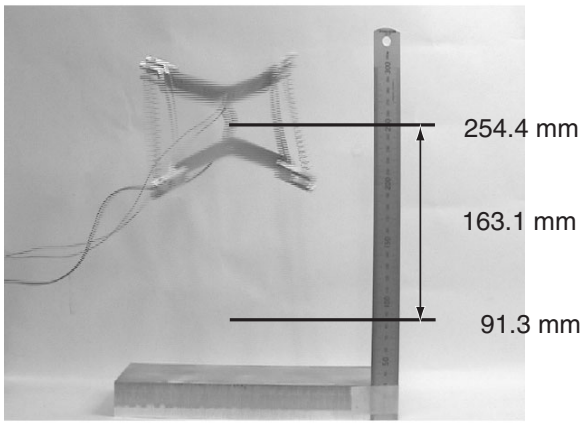

(b)

Fig. 14 Maximum jump heights.

structure. For the resetting cycle, a current of 2 Amps was passed through both resetting actuators and took the structure close to latching, to a configuration with $\psi = 11.6°$. Recall that in Figure 10 the minimum required resetting force becomes higher than the NITi spring force at approximately this value of ψ. Hence, the current was increased to 3 Amp for a short time, to complete the reset cycle.

Discussion

It has been demonstrated that the proposed asymmetrically-bistable monolithic jumping structure behaves as designed and is capable of being remotely tripped and reset by means of NiTi spring actuators. One issue must be addressed: the discrepancies between predicted and actual jump heights.

The jump height prediction based on the assumption that all of the energy difference between the two stable states gets transformed into potential energy considerably over-estimates the jump height observed experimentally. In the case in which the resetting actuators are included, there is broad agreement with the experimental; the remaining difference may be readily explained in terms of additional energy losses which were not included in the calculation. These include non-instantaneous energy transfer, friction between the corner pieces and the ground during takeoff, a horizontal component to the jump trajectory and mass of the connecting wires (it may clearly be seen that the crocodile clips connecting the structure to the power supply are being lifted in Figure 14(a)).

As the energy balance approach is the same in the two cases, it may seem surprising that the same method works much better the latter case. A potential explanation may be found from close examination of Figure 14. Due to the low-speed video camera used there is inevitable blurring, but there is rather clear evidence that in (b) there is internal motion which is not present in (a). This indicates that in the case where the resetting actuators are not present, a significant amount of kinetic energy is lost as internal dynamic oscillation. In the case where the actuators are included, the dynamic behaviour of the structure is altered such that a much reduced proportion of energy is lost to internal resonance.

Conclusions

The proposed asymmetrically bistable structure, consisting of pairs of tape springs and leaf springs, has been shown to work well in practice and to agree reasonably closely with the analysis. Most importantly, it demonstrates the possibility of a fully actuated bistable element, capable of doing useful work, that could potentially be used as a structural component in a binary robotic system. The monolithic nature of the proposed structure, and thus the lack of mechanical articulations and of any sliding parts, is a distinct advantage over previous structures for binary robotic systems.

NiTi springs have been shown to be suitable actuators for the purpose of cycling bistable elements between the stable states. However, when this technology is more mature, it is expected that EPAM actuators and nematic elastomers will be used instead.

It must be remembered that the ability of the structure to jump was intended simply as a demonstration of the structure's ability to do useful work. Ultimately, it should be considered a structural element. The proposed structure has two distinct disadvantages as a structural element: first, its quadrilateral shape makes it difficult to integrate it into conventional rigid structures; second, it has low shear stiffness in its lower energy stable state. Both of these defects must be taken into consideration when designing binary robotic

systems based around this element. A potential design is shown in Figure 15. The shaded quadrilaterals represent the bistable element, the circles represent spherical joints, and the lines represent rigid rod elements. Research in this area is ongoing.

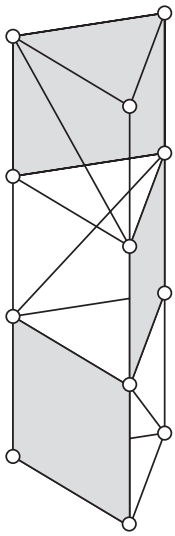

Fig. 15 Concept for binary robotic structure based on an assembly of three asymmetrically-bistable units.

Acknowledgements

Financial support from the Cambridge-MIT Institute (CMI) is gratefully acknowledged. The authors are grateful to Dr E. Terentjev and Professor M. Warner for introducing them to the exciting field of nematic elastomers, and to Dr Terentjev for generously making available several samples.

References

[1]Chirikjian, G.S. "*A binary paradigm for robotic manipulators ",* Proc. of the 1994 IEEE International Conference on Robotics and Automation, pp. 3063-3069, 1994

[2]Schiøler, T., "*Multi-Stability Structures",* Cambridge University First-Year Report, 2002.

[3]Watt, A.M., & Pellegrino, S. "*Tape-spring rolling hinges",* Proc. 36th Aerospace Mechanisms Symposium May 15-17, 2002.

[4]Kornbluh, R., Pelrine, R., Pei, Q., Oh, S. & Joseph, J., "*Ultra-high strain response of field-actuated elastomeric polymers",* Smart Structures and Materials 2000: Electroactive Polymers and Devices, Proc. SPIE, 2000.

[5]Pelrine, R., Kornbluh, R., & Kofod, G., "*High strain actuator materials based on dielectric elastomers",* Advanced Materials, pp 1223-1225, 2000.

[6]Wingert, A., Lichter, M., Dubowsky, D., & Hafez, M., "*Hyper-Redundant Robot Manipulators Actuated by Optimized Binary Dielectric Polymers ",* Proc. of the Society of Photo-Optical Instrumentation Engineers (SPIE) 4695, pp. 415-423, 2002

[7]Terentjev, E. M., "*Liquid-crystalline elastomers",* J. Phys.: Condens. Matter, pp R239-R257, 1999.

[8]Cedrat Technologies. 10, Chemin de Pré Carré– Zirst 38246 MEYLAN Cedex – FRANCE. http://www.cedrat.com

[9]Huang, W., Pellegrino, S. & Bashford, D.P., "*Shape memory actuators for deployable structures ",* Proc. Spacecraft Structures, Materials and Mechanical Testing, pp 53-61, 1996.

[10]Mondotronics Inc. 124 Paul Drive, Suite 12 San Rafael, CA 94903 US. http://www.robotstore.com

[11]Seffen, K.A., & Pellegrino, S. "*Deployment dynamics of tape springs ",* Proc. R. Soc. Lond. A(1999) 455 pp. 1003-1048

[12]Timoshenko, S., & Gere, J., "*Theory of Elastic Stability",* 2nd ed. McGraw-Hill, pp 346-347, 1988.

[13]Matlab Version 6.5. Mathworks Inc. 2002